Pol. J. Environ. Stud. Vol. 34, No. 3 (2025), 2223-2232
DOI: *10.15244/pjoes/187602* ONLINE PUBLICATION DATE: 2024-09-17

Original Research

Adsorption of Methylene Blue Dye by Modified Reed Activated Carbon: Adsorption Optimization and Adsorption Performance

Rurong Jiang[1*], Fang Ren[2]

[1] School of Public Utilities, Jiangsu Urban and Rural Construction Vocational College, Changzhou 213247, China
[2] School of Resources and Environmental Engineering, Jiangsu University of Technology, Changzhou 213001, China

Received: 09 February 2024
Accepted: 18 April 2024

Abstract

To realize the effective utilization of reed for adsorption of methylene blue (MB), modified reed activated carbon (M-RAC) was prepared using reed as raw material and $MgCl_2$ and $FeCl_3$ as activators. The four parameters of M-RAC dosage, MB concentration, adsorption time, and oscillation velocity during the adsorption process were optimized by the response surface methodology (RSM). The adsorption performance of M-RAC on MB under the optimal process was determined and analyzed by three different adsorption models. The results showed that the adsorption capacity of M-RAC on MB was 436.33 mg/g when the M-RAC dosage was 0.17 g, the MB concentration was 550 mg/L, the adsorption time was 105 min, and the oscillation velocity was 154 r/min. The experimental data were consistent with the Langmuir model and Pseudo-second-order kinetics, which indicated that the adsorption process was a monolayer chemical adsorption process. The thermodynamic study confirmed that the increase in temperature favored the adsorption of M-RAC on MB, and the adsorption process was a spontaneous and heat-absorbing reaction. The analysis of the Fourier transform infrared (FTIR) spectroscopy showed that the absorption peaks of hydroxyl functional groups in the prepared M-RAC were higher, and the C-O characteristic peaks were enhanced. The results suggest that M-RAC is a potential biochar adsorbent for effectively removing MB dye from wastewater.

Keywords: adsorption, optimization, modified reed activated carbon (M-RAC), methylene blue (MB), response surface methodology (RSM)

Highlights:

- Methylene blue (MB) adsorption from aqueous solution onto modified reed activated carbon (M-RAC).
- The four parameters of M-RAC dosage, MB concentration, adsorption time, and oscillation velocity during the adsorption process were optimized by the response surface methodology (RSM).
- The experimental data were consistent with the Langmuir model and Pseudo-second-order kinetics.
- The thermodynamic study confirmed that the increase in temperature favored the adsorption of M-RAC on MB.

* e-mail: 010278@jscc.edu.cn
Tel.: 086-183-81388695

Introduction

With the rapid development of the dyestuff industry, the variety of dyestuff is increasing year by year. Methylene blue (MB) dye is a typical cationic dye, often used as a biological stain, especially in the staining of bacteria and cells [1]. Methylene blue is also widely used as a chemical indicator, dye, and drug [2]. Methylene blue dye is alkaline in aqueous solution, toxic, and difficult to degrade in the environment. When methylene blue dye comes into direct contact with people, it may cause damage to the skin, eyes, respiratory system, etc., and may even cause cancer [3]. The current methods for treating MB dye wastewater include coagulation and precipitation, biosorption, membrane separation and advanced oxidation [4-5]. The biosorption approach is widely used in dye wastewater treatment because of its low cost, simple operation, large specific surface area, and high stability compared with the traditional adsorption method [6-7].

Activated carbon is a typical representative of porous carbon materials, which has become one of the most commonly used adsorbents as well as the first porous carbon material to be industrially applied [8]. In recent years, domestic and foreign scholars have begun to study the search for cheap and readily available biomass-activated carbon, such as reed, straw, bark, and nut shells, which have sound adsorption effects [9-10]. The reed straw is a high-quality raw material for preparing activated carbon because of its well-developed aeration tissue and high fiber content, and the straw contains up to 44% carbon [11]. China's reed cultivation area is more than 3 million mu, with a mu output of 500-100 kg and an annual output of more than 3 million tons [12]. Activated carbon prepared from reed can effectively adsorb pollutants such as dyes, heavy metals, and organic matter [13-14]. Zhou et al. [15] prepared activated carbon with high adsorption properties from reeds from the Yellow River Delta. The maximum adsorption capacity of reed activated carbon obtained from the Langmuir isotherm equation was 704.23 mg/g at 30 °C. Its high adsorption capacity can be attributed to its low polarity, multiple surface functional groups, high surface area and pore volume, and layered porous structure. Karoui et al. [16] reported that by developing an enhanced reed biochar as an adsorbent, the removal of MB was 100% at an adsorbent dosage of 1.55 g/L, an MB dosage of 75 mg/L, a pH of 10.42, and a contact time of 115.28 min.

In this study, to further improve the adsorption effect, the reed activated carbon was modified with metal salts. The advantages of metal salt modified adsorbents can improve the pore size structure, improve the stability, and enhance the adsorption performance of some specific pollutants [17]. The disadvantages are that the preparation process is complicated and the cost is high [18]. Among the many metal salts, magnesium chloride and ferric chloride are often used as modifiers for activated carbon based on their efficient modification effect, relatively low cost, and environmental friendliness [19]. Based on the advantages of synergistic effect, modulation of modification effect, and cost reduction when the two modified materials are mixed, the mixture of magnesium chloride and ferric chloride is used to modify the reed activated carbon [20-21].

Therefore, in this paper, the modified reed activated carbon (M-RAC) was prepared and activated by a physicochemical method using $MgCl_2$ and $FeCl_3$ as raw materials and synergistic activation. The effects of M-RAC dosage, MB concentration, adsorption time, and oscillation velocity on MB adsorption were investigated using the Box-Behnken module of Response Surface Methodology (RSM), and the optimized preparation conditions were obtained. Combined with the results of the optimized experimental conditions, the adsorption process of M-RAC on MB was analyzed in depth by adsorption isotherm, adsorption kinetics, and adsorption thermodynamics to provide valuable references for the improvement of the waste utilization of straw and the treatment of MB dye wastewater.

Materials and Methods

Preparation of M-RAC

The M-RAC used in this study was purchased from Yancheng City, Jiangsu Province, China. The dried reed was first cleaned to remove the surface adhesion and then air-dried, and the dried reed was sieved into a porcelain crucible, compacted, sealed with a lid, and put into a muffle furnace and heated to 500 °C at a constant temperature of 7 °C/min for 2 h. After the temperature was reduced to room temperature, it was taken out, milled, and passed through a sieve of 0.15 mm to make the powdered biocarbon.

Reed activated carbon was modified with a mixture of $MgCl_2$ and $FeCl_3$ under the following conditions: room temperature of 25 °C, $MgCl_2$ concentration of 0.5 mol/L, $FeCl_3$ concentration of 0.04 mol/L, pH=4, and the modification time of 24h. 2g of reed biochar was put into a 100 mL vinyl centrifuge tube with a stopper, added with 60 mL of the abovementioned mixture, and shaken well. After this process, put it into the constant temperature oscillator at 25 °C, set the vibration speed of 200 r/min, oscillate for 30 min, soak for 24 h, take out and filter, dry in 105 °C drying oven for 48 h to dry thoroughly, cool down and then store in a sealed bag in the desiccator for spare.

RSM Design

The RSM experiments were designed using the Box-Behnken module in DesignExpert software. The Box-Behnken design requires fewer experiments, has no axial points, and is safer in practice [22]. Based on the results of the previous one-factor experiments, a total of 30 experimental conditions were designed based on the four-factor and three-level experimental design scheme with the four factors of M-RAC dosage (0.06~0.18 g), MB concentration (300~600 mg/L), adsorption time (30~150 min), and oscillation velocity (120-180 r/min) as the independent variables. Quadratic regression analysis was

performed to obtain the optimized adsorption conditions using the adsorption capacity of M-RAC for MB as the response value. The influencing factors and values are shown in Table 1.

Table 1. Experimental factors and levels

Experimental factors		level		
		-1	0	+1
A	M-RAC dosage (g)	0.06	0.12	0.18
B	MB concentration (mg/L)	300	450	600
C	Adsorption time (min)	30	90	150
D	Oscillation velocity (r/min)	120	150	180

Calculation of Adsorption Volume

In this experiment, the adsorption amount of MB was used as an index to evaluate the adsorption performance of M-RAC. The corresponding mass of M-RAC was accurately weighed in an electronic balance and placed in a conical flask containing 250 mL of the corresponding MB concentration. After the adsorption experiment, the conical flask was precipitated for 10 min, and the supernatant was taken and filtered through a 0.45 μm filter membrane. The absorbance of the solution was measured at 470 nm with a UV-visible spectrophotometer. The remaining concentration of MB solution was calculated from the standard curve, and then the adsorbed amount of MB, q, was calculated according to the mass of M-RAC added, as shown in Equation (1).

$$q = \frac{(C_0 - C_1)V}{m} \quad (1)$$

Where q is the adsorption amount of MB, mg/g; C_0 is the concentration of MB solution before adsorption, mg/L; C_1 is the concentration of MB after adsorption, mg/L; V is the volume of solution in the conical flask, L; m is the amount of M-RAC dosage, g.

Adsorption Isotherm Test

In order to gain insight into the adsorption process, the nature of the adsorbent, and the interaction between the adsorbent and the adsorbent, the Langmuir and Freundlich adsorption isotherms were tested. Referring to the optimization results of the response surface, 100 mL of MB solution with concentrations of 50 mg/L, 100 mg/L, 150 mg/L, 200 mg/L, 300 mg/L, 400 mg/L, 500 mg/L, and 700 mg/L were added to eight 250 mL order conical flasks with 0.12 g of M-RAC at 288 K, 298 K and 308 K at three temperatures, and the adsorption isotherms were studied by oscillating in a water bath shaker at 150 r/min for 105 min.

Two commonly used isothermal adsorption models, Langmuir and Freundlich, were chosen to fit the experimental data with linear and nonlinear data. The linear expressions of these two equations are shown in (2) and (3), respectively.

$$q_e = \frac{q_m K_L C_e}{1 + K_L C_e} \quad (2)$$

$$q_e = K_F C_e^{\,1/n} \quad (3)$$

Where the q_e is the adsorption amount at equilibrium time, mg/g; C_e is the concentration of the remaining MB when the adsorption reaches equilibrium, L/mg; K_F is the adsorption equilibrium constant of the Freundlich model, denoting the adsorption capacity; n is the Freundlich constant, denoting the adsorption strength and adsorption rate. When $1/n$ is equal to 0~1, it indicates that the adsorption process is easy to carry out, and when $1/n > 1$, it indicates that the adsorption process is challenging to carry out.

Adsorption Kinetics Test

Concerning the optimization results of the response surface, 100 mL of MB solution at a concentration of 450 mg/L was added to each of the 11 sets of 250 mL conical flasks. Then 0.12 g of M-RAC was added, and the flasks were oscillated in a water-bath shaker at a speed of 150 r/min. Samples were taken at 5, 10, 20, 30, 50, 70, 90, 120, 150, 180 and 240 min for adsorption kinetic studies.

The commonly used Pseudo-first-order and Pseudo-second-order kinetic models were selected for fitting and analyzing the experimental data, and the fitting equations are shown in Equations (4) and (5), respectively.

$$q_t = q_e(1 - e^{-k_1 t}) \quad (4)$$

$$q_t = \frac{k_2 q_e^{\,2} t}{1 + k_2 q_e t} \quad (5)$$

Where t is the contact time, min; q_e is the amount of M-RAC adsorbed at equilibrium, mg/g; q_t is the amount of M-RAC adsorbed at time t, mg/g; k_1 is rate constant for Pseudo-first-order kinetics, min^{-1}; k_2 is rate constant for Pseudo-second-order kinetics, g/(mg-min).

Adsorption Thermodynamics

In order to gain insight into the nature of the adsorption process, the adsorption of M-RAC on MB was thermodynamically investigated to understand the energy changes at different temperatures. The thermodynamic parameters determined were Gibbs free energy (ΔG^0, kJ/mol), enthalpy change (ΔH^0), and entropy change (ΔS^0, J/(mol·K)). Thermodynamic calculations of the M-RAC adsorption MB process were performed using Equation (6-8) [23].

$$K_c = \frac{C_{ad}}{C_e} \quad (6)$$

$$\Delta G^0 = -RTlnK_c \quad (7)$$

$$\Delta G^0 = \Delta H - T\Delta S \quad (8)$$

Where K_c is the thermodynamic equilibrium constant; C_{ad} is the concentration of adsorbate on the adsorbent at adsorption equilibrium, mg/L; C_e is the concentration of residual MB at adsorption equilibrium, mg/L;ΔG^0 is the Gibbs free energy, kJ/mol; R is the gas constant, 8.314 J/

(mol·K); T is the absolute temperature, K; and ΔH^0 is the enthalpy change of adsorption, kJ/ mol; ΔS is the entropy change of adsorption, J /(mol·K).

Analysis Method

The MB concentration was determined at a maximum wavelength of 470 nm using a UV-VIS spectrophotometer (Alpha-1506, Shanghai Puyuan, China). The response surface test design, regression equation, and optimization analysis were performed using Design Expert (8.0.6, Stat-Ease Inc, USA) software. Graphs of adsorption properties were plotted using origin (2022, Electronic Arts Inc, USA).

Results and Discussion

Optimization of Adsorption Parameters

Adsorption Capacity and Variance Analysis

The results of the RSM experimental design for specific working conditions and corresponding response values are shown in Table 2. In order to investigate the effects of M-RAC dosage, MB concentration, adsorption time, and oscillation velocity on the removal of MB dye by M-RAC adsorption, multiple quadratic regressions were fitted to the data using Design Expert, and ANOVA analyzed the resulting model results. The regression equation for this experiment is shown in Equation (6).

$$Y = 377.68 + 37.82X_1 + 36.21X_2 + 24.14X_3 + 11.56X_4 - 11.40X_1X_2 + 9.88X_1X_3 + 6.58X_1X_4 + 2.03X_2X_3 + 15.19X_2X_4 - 1.77CD - 8.23X_1^2 - 0.0005.417X_2^2 - 102.44X_3^2 - 29.88X_4^2 \quad (6)$$

The positive coefficients of all four factors in Equation (2) indicate that all four factors can cause an increase in the adsorption value. In the interaction, the negative coefficients of factors X_1 and X_2, X_3 and X_4 indicate that they can cause a decrease in the response value.

Analysis of variance was performed on the model, and the results showed that F =57.94, P<0.0001, reached a highly significant level ($P \leq 0.01$) in the constructed regression model. Lack of fit was not significant (P =0.5242>0.05), indicating that the model was reliable [24]. The R-squared was 98.18%>85%, indicating that the model fits well with the experimental results. Its predicted values can replace the experimental values in describing the relationship between the factors and the response values. The Adj R^2 was = 0.9649,

Table 2. Experimental design and adsorption capacity analysis

Numbers	Actual values				Coded values				Measured value Y (mg/g)	Predicted value (mg/g)
	X_1	X_2	X_3	X_4	X_1	X_2	X_3	X_4		
1	0.06	450	90	120	-1	0	0	-1	307.95	310.34
2	0.12	600	90	180	0	1	0	1	410.27	406.25
3	0.12	450	90	150	0	0	0	0	369.75	373.49
4	0.18	450	30	150	1	0	-1	0	273.51	280.76
5	0.12	600	30	150	0	1	-1	0	284.65	291.17
6	0.12	600	90	120	0	1	0	-1	354.55	364.86
7	0.12	450	30	120	0	0	-1	-1	199.57	194.96
8	0.18	450	150	150	1	0	1	0	326.19	321.24
9	0.06	450	90	180	-1	0	0	1	299.85	297.96
10	0.06	450	30	150	-1	0	-1	0	221.85	213.63
11	0.06	450	150	150	-1	0	1	0	235.02	235.47
12	0.18	450	90	180	1	0	0	1	392.03	406.28
13	0.12	450	150	120	0	0	1	-1	250.21	247.60
14	0.12	450	90	150	0	0	0	0	364.68	365.86
15	0.12	450	30	180	0	0	-1	1	242.11	240.98
16	0.12	300	30	150	0	-1	-1	0	208.68	214.63
17	0.12	300	150	150	0	-1	1	0	269.46	275.51
18	0.12	300	90	120	0	-1	0	-1	309.98	306.64
19	0.12	450	150	180	0	0	1	1	285.67	287.77
20	0.12	450	90	150	0	0	0	0	375.82	361.10
21	0.12	300	90	180	0	-1	0	1	304.91	301.72
22	0.12	600	150	150	0	1	1	0	353.54	359.53
23	0.12	450	90	150	0	0	0	0	393.04	394.61
24	0.06	300	90	150	-1	-1	0	0	287.69	278.20
25	0.12	450	90	150	0	0	0	0	392.03	397.09
26	0.18	600	90	150	1	1	0	0	426.47	410.15
27	0.12	450	90	150	0	0	0	0	370.76	384.09
28	0.18	450	90	120	1	0	0	-1	373.80	359.03
29	0.18	300	90	150	1	-1	0	0	386.97	401.27
30	0.06	600	90	150	-1	1	0	0	372.78	374.51

and the difference with R^2 was less than 0.2, indicating that the model is reasonable. The coefficient of variation is 3.77%<10%, which indicates that the non-experimental factors are weakly interfering and the experimental stability of the model is good [25]. Therefore, this Equation can be used to analyze and predict the effects of various factors on the adsorption of MB by M-RAC.

It can be seen that the primary terms X_1, X_2, X_3, X_4 and the interaction terms X_1 X_2, X_2 X_4, X_3^2, and X_4^2 had significant effects on the adsorption capacity of M-RAC by the sum of squares statistics. In addition, from the sum of squares of different factors in Table 3, it can be seen that the order of the four factors on the adsorption capacity of M-RAC adsorption for MB was as follows: the M-RAC dosage > MB concentration > adsorption time > oscillation velocity.

Parameters Interaction Analysis

According to ANOVA, it is clear that in the interaction of four factors, the P value is less than 0.05, only factors X_1 X_2 (0.0458), X_2 X_4 (0.0243). Therefore, the response surface analysis was performed only for these two groups of factors. The three-dimensional graphs and two-dimensional contour plots of the interaction between M-RAC dosage and MB concentration on MB adsorption are shown in Fig. 1. The positive effects of M-RAC dosage and MB concentration on the experimental results are shown in Fig. 1. The M-RAC dosage and MB concentration positively affected the experimental results. The MB adsorption amount showed an increasing trend with the increase of M-RAC dosage and MB concentration. The maximum MB adsorption was observed when the

Table 3. Response surface model results and variance analysis

Source	Sum of squares	Df	Mean square	F value	P value Prob > F
Model	119366.41	14	8526.17	57.94	< 0.0001
X_1	17163.02	1	17163.02	116.62	< 0.0001
X_2	15738.10	1	15738.10	106.94	< 0.0001
X_3	6994.08	1	6994.08	47.52	< 0.0001
X_4	1604.71	1	1604.71	10.90	0.0048
X_1 X_2	519.50	1	519.50	3.53	0.0458
X_1 X_3	390.20	1	390.20	2.65	0.1243
X_1 X_4	173.42	1	173.42	1.18	0.2948
X_2 X_3	16.42	1	16.42	0.11	0.7430
X_2 X_4	923.55	1	923.55	6.28	0.0243
X_3 X_4	12.52	1	12.52	0.09	0.7745
X_1^2	464.59	1	464.59	3.16	0.0959
X_2^2	0.00	1	0.00	0.00	0.9999
X_3^2	71956.49	1	71956.49	488.95	< 0.0001
X_4^2	6123.15	1	6123.15	41.61	< 0.0001
Residual	2207.50	15	147.17		
Lack of fit	1482.17	10	148.22	1.02	0.5242
Pure error	725.33	5	145.07		
Cor total	121573.91	29			

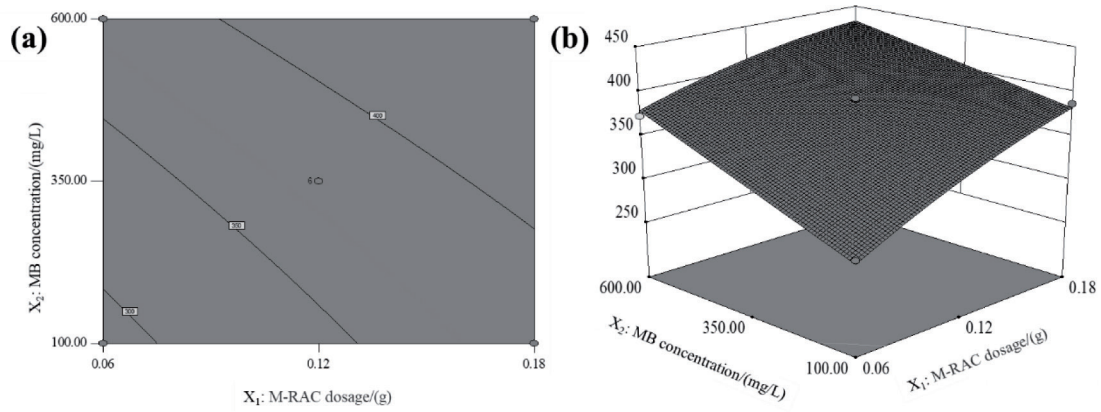

Fig. 1. Three-Dimensional Graphs and Two-Dimensional Contour Plots for the factor X_1 and X_2

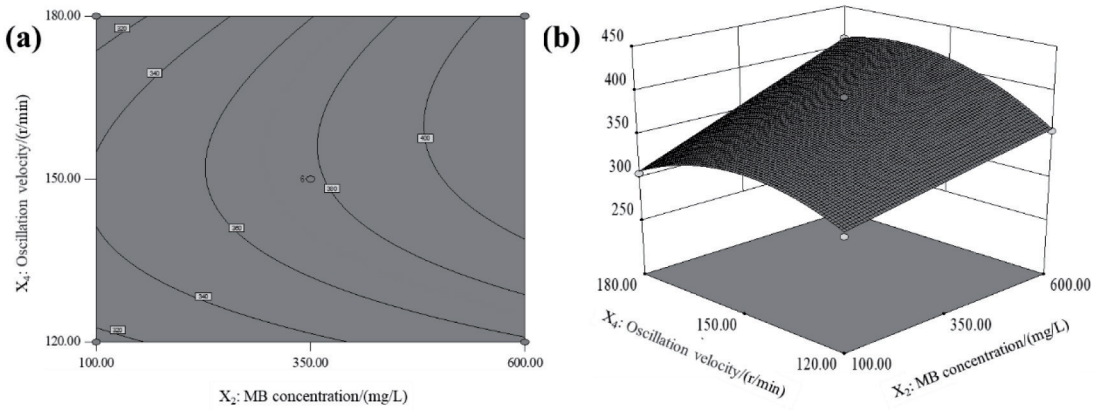

Fig. 2. Three-Dimensional Graphs and Two-Dimensional Contour Plots for the factor X_2 and X_4

M-RAC dosage was 0.18 g, and the MB concentration was 600 mg/L (experimental condition 26). The increase of M-RAC dosage, on the one hand, led to the introduction of more adsorption active sites, which made the contact area between the M-RAC and MB increase, and on the other hand, made the diffusion resistance of MB on the surface of the M-RAC decrease, which was favorable to the adsorption of MB [26-27]. However, an excess of M-RAC may also lead to an increase in the resistance of the activated carbon bed and subsequently weaken the adsorption of MB.

Three-Dimensional Graphs and Two-Dimensional Contour Plots of the effect of the interaction of MB concentration and oscillation velocity are shown in Fig. 2. With the increase of MB concentration, the MB adsorption amount showed an increasing trend. However, the best adsorption of MB by M-RAC was observed when the oscillation velocity was at 150 r/min, and the adsorption effect was not as good as the median value when the oscillation velocity was equal to 120 r/min and 180 r/min. The diffusion coefficient of MB on the surface of M-RAC may increase when the oscillation velocity is too large, making it difficult for MB to stay on the surface of M-RAC for a sufficient period and affecting the adsorption effect [28]. The contact time between M-RAC and MB may not be sufficient when the oscillation velocity is too low, and the diffusion coefficient of MB on the surface of M-RAC may be smaller, thus affecting the adsorption effect [29].

Optimization Validation

The optimal adsorption levels of the four factors for the adsorption of MB dye by M-RAC were obtained by the optimization module in the Design-Experts 8. 0. 6 software: M-RAC dosage of 0.17 g, MB concentration of 550 mg /L, adsorption time of 105 min, oscillation velocity of 154 r/min.

The average adsorption capacity of M-RAC for MB under this optimal adsorption condition was 436.33 mg/g. In order to test the reliability of the optimal adsorption capacity of M-RAC, three parallel experiments were carried out under the optimal adsorption level of the four factors. The validation results showed that the average adsorption capacity of M-RAC for MB under the optimal adsorption level was 427.17 mg/g, with an error of 2.06% from the predicted value, indicating that the test results based on the present RSM method were accurate and reliable. Compared with the results of other literature, the removal rate of MB is moderately high [13, 15-16].

Adsorption Isotherms

The initial concentration of MB was 50-600 mg/L, and the dosage of M-RAC was 1.2 g/L. The conical flasks were shaken at 150 r/min for 105 min to adsorption equilibrium in a constant temperature water bath shaker. The adsorption performance of M-RAC on MB was examined at different MB concentrations and temperatures.

Fig. 3 shows the adsorption change process of M-RAC on MB at three different temperatures, 288, 298, and 308 K. The adsorption of M-RAC on MB is shown in Fig. 3 and Table 4. From Fig. 3 and Table 4, it can be seen that the adsorption of MB by M-RAC increased gradually with

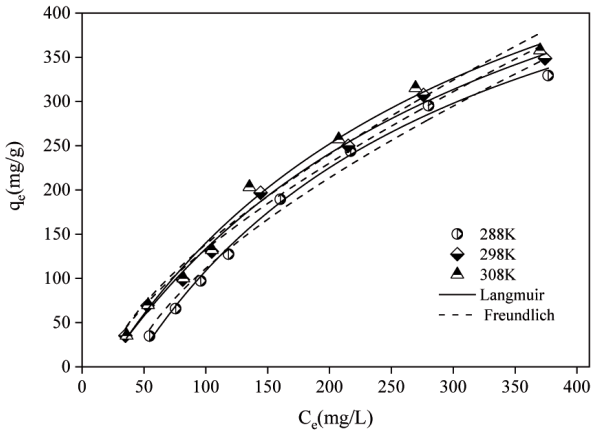

Fig. 3. Nonlinear fitted curve with isotherm models

Table 4. Parameters of isotherm model at different temperatures

Temperature/K	Langmuir			Freundlich		
	Q_m (mg/g)	K_L (L/mg)	R^2	K_F	n	R^2
288	413.08	0.0060	0.9956	10.50	1.52	0.9807
298	484.90	0.0059	0.9943	10.52	1.47	0.9856
308	491.61	0.0065	0.9897	11.66	1.48	0.9768

Table 5. Adsorption kinetic parameters of MB by M-RAC

Temperature/K	Pseudo-first-order			Pseudo-second-order		
	$q_{e,cal}$ (mg/g)	k_1 $(min)^{-1}$	R^2	$q_{e,cal}$ (mg/g)	k_2 $(g\text{-}mg^{-1}\cdot min)^{-1}$	R^2
288	278.14	0.0283	0.9798	331.13	0.000091	0.9983
298	310.90	0.0292	0.9827	358.33	0.000097	0.9969
308	332.85	0.0310	0.9850	372.87	0.000105	0.9860

increasing temperature, which indicates that the adsorption process is heat-absorbing (Fig. 4). The increase in temperature promotes the adsorption process. In comparing the two models, the correlation coefficients R^2 obtained from the Langmuir model at different temperatures were 0.9956, 0.9943, and 0.9897, while those of the Freundlich model were 0.9807, 0.9856, and 0.9768. Although the correlation coefficients of the two models were higher, the Langmuir model had a better fitting effect. It indicates that the Langmuir model can better simulate the adsorption process of M-RAC on MB. It can be seen that the adsorption of M-RAC on MB occurs on the surface of the adsorbent, and the adsorption is dominated by monolayers, with few multilayers stacking or aggregation, as well as few interactions or competitions between MB molecules [30]. In the Freundlich model, the K_F value showed a positive correlation with the temperature (Table 4), indicating that the adsorption capacity of M-RAC was enhanced by the increase in temperature, which also indicated that the adsorption of MB by M-RAC was a heat-absorbing process.

Adsorption Kinetics

In the kinetic experiments, the initial concentration of MB was 450 mg/L, and the dosage of M-RAC was 1.2 g/L. The effects of different temperatures and adsorption times on the adsorption process of MB were examined (Fig. 5). As shown in Table 5, the $q_{e,cal}$ value (the theoretical value of q_e) of the Pseudo-first-order kinetic model was lower than the actual value, and the correlation coefficient was slightly lower than that of the Pseudo-second-order kinetic model, which indicated that the Pseudo-first-order kinetic model was not suitable for describing the adsorption process of M-RAC on MB. The $q_{e,cal}$ values of the Pseudo-second-order kinetic model are closer to the actual values, and the correlation coefficients are above 0.98, indicating that this model is more suitable for describing the adsorption process of M-RAC on MB (Fig. 6). In the adsorption process of M-RAC on MB, physical adsorption and diffusion are complementary, and chemical adsorption is dominant [31]. This adsorption process may involve: 1) the formation of ions or dipole molecules between dye molecules and M-RAC through electron transfer; 2) the ions in MB may complex with some ions on the surface of reed activated carbon to form stable complexes; 3) the hydroxyl or other groups on the surface of reed activated carbon may form hydrogen bonds with MB molecules, which results in adsorption [32-33]. The k and $q_{e,cal}$ values of the Pseudo-first-order and Pseudo-second-order kinetic models increased with the adsorption temperature, indicating that warming could accelerate the adsorption of MB by M-RAC.

Adsorption Thermodynamics

In Table 6, $\Delta G^0<0$ indicates that the process of MB adsorption by M-RAC is spontaneous. When the temperature was incremented, ΔG^0 increased from -17.68 kJ /mol to -18.73 kJ /mol and -19.59 kJ /mol, suggesting that increasing the temperature promotes the adsorption [34]. The ΔH^0=16.76 kJ/mol, indicating that the adsorption process absorbs heat and that increasing the temperature facilitates the adsorption, which agrees with experimental

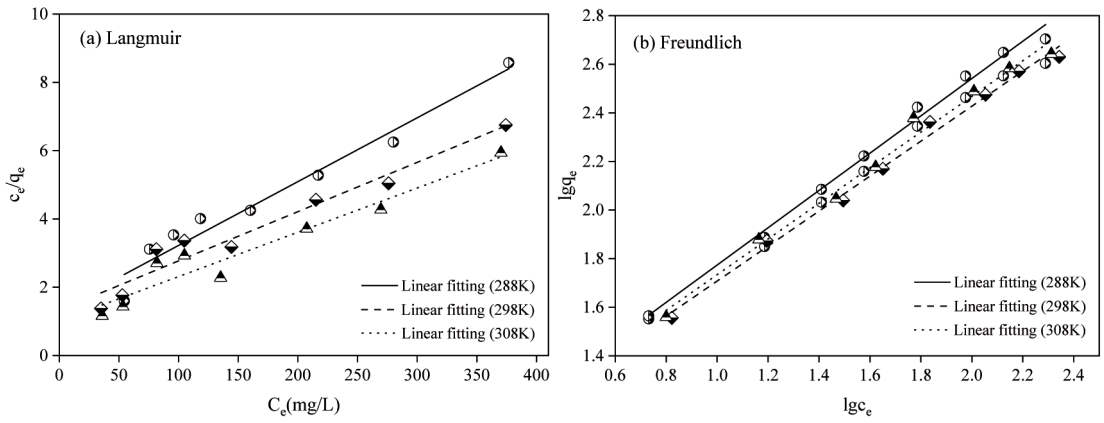

Fig. 4. Linear fitted curve with isotherm models

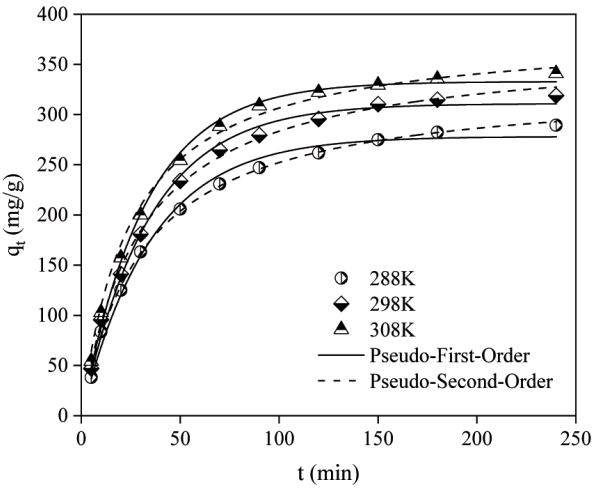

Fig. 5. Regression curves for the adsorption of MB by M-RAC

Table 6. Thermodynamic parameters for the adsorption of MB on M-RAC

Temperature (k)	ΔG^0 (kJ/mol)	ΔH^0 (kJ/mol)	ΔS^0 (kJ·mol·K)$^{-1-1}$
288	-17.68	16.76	0.9536
298	-18.73		
308	-19.59		

results of adsorption isotherm. The ΔS^0=0.9536 kJ·mol^{-1}K^{-1}, indicating that the degree of freedom of the solid-liquid surface increases during adsorption [35]. The above experimental data indicated that the adsorption of MB by M-RAC proceeded spontaneously and was accompanied by an increase in the system's energy.

FTIR Analysis

In the adsorption kinetic analysis, it is known that the Pseudo-second-order kinetic model is more suitable to describe the adsorption of MB by M-RAC. Therefore, the activated carbon surface was explored for chemical group changes by performing an FTIR spectroscopy analysis of the original RAC and M-RAC.

The surface functional groups of original reed biochar and activated charcoal are similar but slightly different (Fig. 7). 3439 cm-¹ is the location of the hydroxyl (-OH) stretching vibration peak, which is shown to be sharp and intense, indicating the presence of free hydroxyl groups in the molecule [36]. Near 2349 cm-¹ corresponds to the free C-H stretching vibration absorption peak. Near 1645 cm-¹, this wave number is usually associated with C=O stretching vibrations, such as carboxyl, ester groups, etc. Near 1081 cm-¹, this wave number is usually associated with C-O stretching vibration, such as alcohols, phenols, ethers, etc. [37]. The M-RAC has a significant absorption peak near 3439 cm-¹, which suggests that the chloride ions may be chemically reacted with the hydroxyl group and other functional groups on the surface of the activated carbon in the process of preparing activated carbon at high temperatures with the powder of reed straw—chemical reaction. Compared with the original carbon, the characteristic peak near 1081 cm^{-1} of M-RAC is enhanced, indicating that the modification process generated more C-O stretching vibration absorption peaks.

Conclusions

(1) The experimental results of the RSM showed that the optimal adsorption parameters of modified reed activated carbon were: M-RAC dosage of 0.17 g, MB concentration of 550 mg/L, adsorption time of 105 min, and oscillation velocity of 154 r/min. Under these conditions, the adsorption capacity of MB by M-RAC was 436.33 mg/g, and the error with the predicted value was 2.06%, which indicated that the experimental results based on the present RSM method were accurate and reliable.

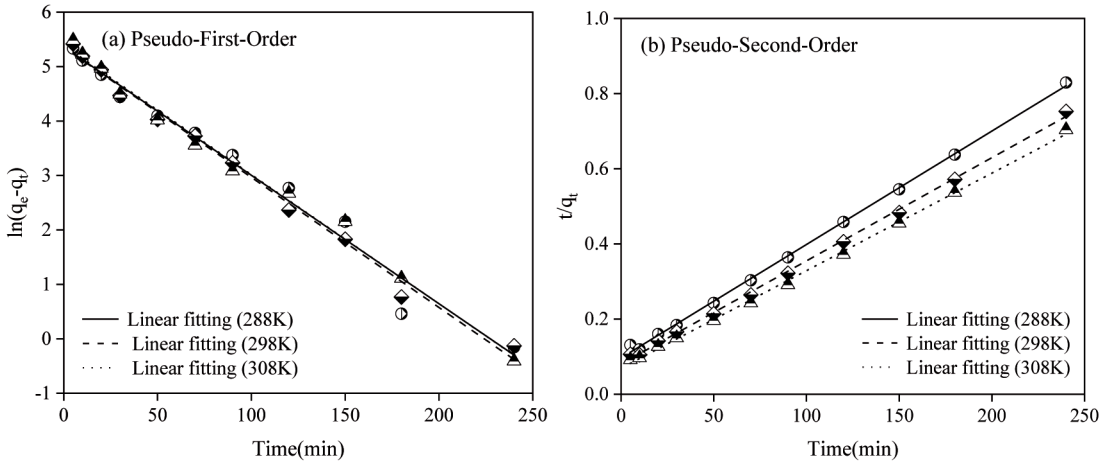

Fig. 6. Adsorption kinetics of MB by M-RAC

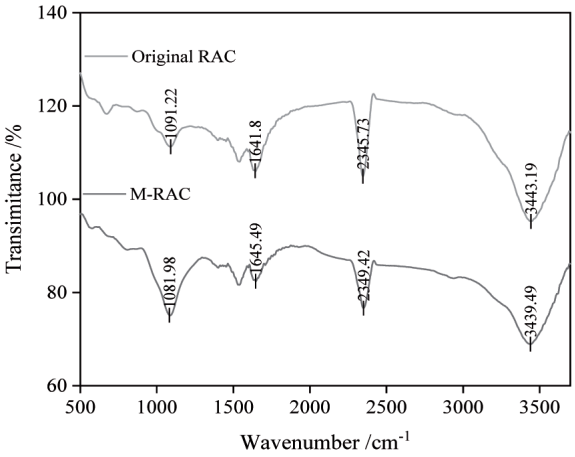

Fig. 7. FTIR spectra of the original RAC and M-RAC

(2) The theoretical maximum adsorption of MB by Langmuir isothermal adsorption curve at 308 K temperature was 491.61 mg/g (R^2 =0.9897), which was better fitted with the adsorption process. The secondary kinetic adsorption curve can better describe the adsorption kinetic process of M-RAC on MB (R^2>0.9800). The adsorption thermodynamics indicated that the thermodynamic results showed that the adsorption process was spontaneous ($-\Delta G^0$), heat absorption (ΔH=16.76), entropy increase (ΔS=0.9536), and dominated by chemisorption.

(3) The results of FTIR analysis showed that the absorption peaks of hydroxyl functional groups in the prepared M-RAC were more apparent. In contrast, the C-O characteristic peaks were enhanced compared with those before modification. The results of the adsorption study validate the M-RAC as a suitable adsorbent for water treatment.

Acknowledgments

This work was supported by the funding provided by the Science and Technology Planning Project of Changzhou (CJ20210054).

Conflict of Interest

The authors declare no conflict of interest.

References

1. LI S., CHEN H., LI Y., DU Z., BIN L., LI W., FU F., LI P., TANG B. Efficient removal of refractory dyestuffs from textile wastewater by composite hydrated alumina derived from waste aluminum polishing solution. Journal of Environmental Chemical Engineering, **11** (3)**,** 109859**, 2023**.
2. SONG Y., WANG L., QIANG X., GU W., MA Z., WANG G. An overview of biological mechanisms and strategies for treating wastewater from printing and dyeing processes. Journal of Water Process Engineering, **55,** 104242**, 2023**.
3. GEBRE MESKEL A., KWIKIMA M.M., MESHESHA B.T., HABTU N.G., NAIK S.V.C.S., VELLANKI B.P. Malachite green and methylene blue dye removal using modified bagasse fly ash: Adsorption optimization studies. Environmental Challenges, **14,** 100829**, 2024**.
4. JIANG R., YAO J., YAO Y. Optimization of The Modified Soybean Straw Activated Carbon for Adsorption of Methylene Blue Dye by Response Surface Methodology. Polish Journal of Environmental Studies, **32** (5)**,** 4073**, 2023**.
5. HASSANZADEH H., SALEM A., SALEM S. Fabrication of MgO powder through ultrasound-assisted precipitation for uptake of reactive dyes from wastewater: Change in porous structure for efficient adsorption. Inorganic Chemistry Communications, **155,** 111004**, 2023**.
6. YE H., CHEN D., LI N., XU Q., LI H., HE J., LU J. Azine-linked covalent organic framework-modified GO membrane for high-efficiency separation of aqueous dyes and salts in wastewater. Journal of Membrane Science, **655,** 120546**, 2022**.
7. ELGARAHY A.M., ELWAKEEL K.Z., MOHAMMAD S.H., ELSHOUBAKY G.A. A critical review of biosorption of dyes, heavy metals and metalloids from wastewater as an efficient and green process. Cleaner Engineering and Technology, **4,** 100209**, 2021**.
8. KUMAR N., PANDEY A., ROSY SHARMA Y.C. A review on sustainable mesoporous activated carbon as adsorbent for efficient removal of hazardous dyes from industrial wastewater. Journal of Water Process Engineering, **54,** 104054**, 2023**.
9. TOMIN O., VAHALA R., YAZDANI M.R. Synthesis and efficiency comparison of reed straw-based biochar as a mesoporous adsorbent for ionic dyes removal. Heliyon, **10** (2)**,** e24722**, 2024**.
10. GAO Y., ZHANG J., CHEN C., DU Y., TENG G., WU Z. Functional biochar fabricated from waste red mud and corn straw in China for acidic dye wastewater treatment. Journal of Cleaner Production, **320,** 128887**, 2021**.
11. WANG H., XU J., LIU X., SHENG L. Preparation of straw activated carbon and its application in wastewater treatment: A review. Journal of Cleaner Production, **283,** 124671**, 2021**.
12. QU F., YU J., DU S., LI Y., LV X., NING K., WU H., MENG L. Influences of anthropogenic cultivation on C, N and P stoichiometry of reed-dominated coastal wetlands in the Yellow River Delta. Geoderma, **235-236,** 227**, 2014**.
13. BOUBAKER H., BEN ARFI R., MOUGIN K., VAULOT C., HAJJAR S., KUNNEMAN P., SCHRODJ G., GHORBAL A. New optimization approach for successive cationic and anionic dyes uptake using reed-based beads. Journal of Cleaner Production, **307,** 127218**, 2021**.
14. Di FIDIO N., LICURSI D., PUCCINI M., VITOLO S., RASPOLLI GALLETTI A.M. Closing a biorefinery cycle of giant reed through the production of microporous and reusable activated carbon for CO2 adsorption. Journal of Cleaner Production, **428,** 139359**, 2023**.
15. ZHOU L., YU Q., CUI Y., XIE F., LI W., LI Y., CHEN M. Adsorption properties of activated carbon from reed with a high adsorption capacity. Ecological Engineering, **102,** 443**, 2017**.
16. KAROUI S., BEN ARFI R., MOUGIN K., GHORBAL A., ASSADI A.A., AMRANE A. Synthesis of novel biocomposite powder for simultaneous removal of hazardous ciprofloxacin and methylene blue: Central composite design, kinetic and isotherm studies using Brouers-Sotolongo family models. Journal of Hazardous Materials, **387,** 121675**, 2020**.

17. WANG Z., NIE Q., LEI Z., ZHANG Z., SHIMIZU K., YUAN T. Enhanced Pb(II) removal from wastewater by co-pyrolysis biochar derived from sewage sludge and calcium sulfate: Performance evaluation and quantitative mechanism analysis. Separation and Purification Technology, **329,** 125124**, 2024**.
18. SUN M., WANG X., XIONG R., CHEN X., ZHAI L., WANG S. High-performance biochar-loaded MgAl-layered double oxide adsorbents derived from sewage sludge towards nanoplastics removal: Mechanism elucidation and QSAR modeling. Science of the Total Environment, **901,** 165971**, 2023**.
19. HOU J., HUANG L., YANG Z.M. Adsorption of ammonium on biochar prepared from giant reed. Environmental Science and Pollution Research, **23** (19), 19107, **2016**.
20. CHENG S., MENG W., XING B. Efficient removal of heavy metals from aqueous solutions by Mg/Fe bimetallic oxide-modified biochar: Experiments and DFT investigations. Journal of Cleaner Production, **403**, 136821, **2023**.
21. MOED N.M., KU Y. Regeneration of As(V) loaded granular activated carbon through desorption in $FeCl_3$, $CaCl_2$ and $MgCl_2$ aqueous solutions. Water Science and Technology, **86** (5), 1253, **2022**.
22. BOUBAKER H., BEN ARFI R., MOUGIN K., VAULOT C., HAJJAR S., KUNNEMAN P., SCHRODJ G., GHORBAL A. New optimization approach for successive cationic and anionic dyes uptake using reed-based beads. Journal of Cleaner Production, **307,** 127218**, 2021**.
23. LIU L. A comprehensive model of adsorption of resorcinol in rotating packed bed: Theoretical, isotherm, kinetics and thermodynamics. Journal of Environmental Chemical Engineering, **11** (5)**,** 111041**, 2023**.
24. MOKHTAR A., ABDELKRIM S., BOUKOUSSA B., HACHEMAOUI M., DJELAD A., SASSI M., ABBOUD M. Elimination of toxic azo dye using a calcium alginate beads impregnated with NiO/activated carbon: Preparation, characterization and RSM optimization. International Journal of Biological Macromolecules, **233,** 123582**, 2023**.
25. OFGEA N.M., TURA A.M., FANTA G.M. Activated carbon from H3PO4 -activated Moringa Stenopetale Seed Husk for removal of methylene blue: Optimization using the response surface method (RSM). Environmental and Sustainability Indicators, **16,** 100214**, 2022**.
26. CHAN A.A., ABDUL RAMAN A.A., CHONG W.L., BUTHIYAPPAN A. Graphene oxide impregnated activated carbon derived from coconut shell through hydrothermal carbonization for cationic dye removal: Adsorptive performance, kinetics, and chemistry of interaction. Journal of Cleaner Production, **437,** 140655**, 2024**.
27. WANG Y., ZHANG Y., LI S., ZHONG W., WEI W. Enhanced methylene blue adsorption onto activated reed-derived biochar by tannic acid. Journal of Molecular Liquids, **268,** 658**, 2018**.
28. LI Y., ZHANG Y., ZHANG Y., WANG G., LI S., HAN R., WEI W. Reed biochar supported hydroxyapatite nanocomposite: Characterization and reactivity for methylene blue removal from aqueous media. Journal of Molecular Liquids, **263,** 53**, 2018**.
29. BOUBAKER H., BEN ARFI R., MOUGIN K., VAULOT C., HAJJAR S., KUNNEMAN P., SCHRODJ G., GHORBAL A. New optimization approach for successive cationic and anionic dyes uptake using reed-based beads. Journal of Cleaner Production, **307,** 127218**, 2021**.
30. de OLIVEIRA T.F., de SOUZA C.P., LOPES-MORIYAMA A.L., PEREIRA DA SILVA M.L. In situ modification of MCM-41 using niobium and tantalum mixed oxide from columbite processing for methylene blue adsorption: Characterization, kinetic, isotherm, thermodynamic and mechanism study. Materials Chemistry and Physics, **294,** 127011**, 2023**.
31. BAZAN-WOZNIAK A., NOSAL-WIERCIŃSKA A., YILMAZ S., PIETRZAK R. Chitin-based porous carbons from Hermetia illucens fly with large surface area for efficient adsorption of methylene blue; adsorption mechanism, kinetics and equilibrium studies. Measurement, **226,** 114129**, 2024**.
32. DEIVASIGAMANI P., SENTHIL KUMAR P., SUNDARAMAN S., SOOSAI M.R., RENITA A.A., KARTHIKEYAN M., BEKTENOV N., BAIGENZHENOV O., VENKATESAN D., KUMAR J.A. Deep insights into kinetics, optimization and thermodynamic estimates of methylene blue adsorption from aqueous solution onto coffee husk (Coffee arabica) activated carbon. Environmental Research, **236,** 116735**, 2023**.
33. JOSHIBA G.J., KUMAR P.S., RANGASAMY G., NGUEAGNI P.T., POOJA G., BALJI G.B., ALAGUMALAI K., EL-SEREHY H.A. Iron doped activated carbon for effective removal of tartrazine and methylene blue dye from the aquatic systems: Kinetics, isotherms, thermodynamics and desorption studies. Environmental Research, **215,** 114317**, 2022**.
34. BOUCHELKIA N., TAHRAOUI H., AMRANE A., BELKACEMI H., BOLLINGER J., BOUZAZA A., ZOUKEL A., ZHANG J., MOUNI L. Jujube stones based highly efficient activated carbon for methylene blue adsorption: Kinetics and isotherms modeling, thermodynamics and mechanism study, optimization via response surface methodology and machine learning approaches. Process Safety and Environmental Protection, **170,** 513**, 2023**.
35. AMRAN F., ZAINI M.A.A. Sodium hydroxide-activated Casuarina empty fruit: Isotherm, kinetics and thermodynamics of methylene blue and congo red adsorption. Environmental Technology & Innovation, **23,** 101727**, 2021**.
36. YAACOUBI F.E., SEKKOURI C., ENNACIRI K., RABICHI I., IZGHRI Z., BAÇAOUI A., YAACOUBI A. Synthesis of composites from activated carbon based on olive stones and sodium alginate for the removal of methylene blue. International Journal of Biological Macromolecules, **254,** 127706**, 2024**.
37. ULFA M., PERTIWI Y.E., SARASWATI T.E., BAHRUJI H., HOLILAH H. Synthesis of iron triad metals-modified graphitic mesoporous carbon for methylene blue photodegradation. South African Journal of Chemical Engineering, **45,** 149**, 2023**.